

# Chapter 22

## Acoustic Cavity Modal Analysis for NVH Development of Road Machinery Cabins

Hongan Xu, Owen Dickinson, John Wang, and Hyunseok Kang

**Abstract** Noise and vibration comfort is a critical design criterion for road machinery. An acoustic modal analysis provides useful insights to understanding interior acoustic characteristics and to developing noise mitigation strategies, to improve operator comfort. In this study, an acoustic cavity modal analysis of a compactor cabin is done by utilizing analytical solution, FEA and experimental measurements. While the analytical method and FEA calculate the normal modes of a rigid-walled acoustic cavity, the physical test measures the acoustic modes *in-situ* that account for the vibro-acoustic coupling effect between the interior cavity and flexible panels. The discrepancies of resultant modal parameters extracted by testing and simulation are discussed. In addition, the impacts of the seat and steering column assembly on the acoustic cavity modes are also investigated. Last but not least, a local vibro-acoustic behavior of the cab and its relation to the interior booming noise is deeply investigated. From the NVH development standpoint for a practical cabin, the findings of this investigation not only help troubleshooting cabin noise issues but also lead to improvement in virtual acoustical modal predictions and guide the design to achieve a robust NVH performance.

**Keywords** Road machinery cabins • Acoustic transfer function • Low frequency booming noise • Acoustic cavity modal analysis • Panel-cavity coupling • Panel resonance

### 22.1 Introduction

The cabin acoustic comfort is one of the most important factors that affect an operator's work environment. As the legal regulations become more and more stringent to limit the interior noise level of construction equipment, designing a quiet cabin appear more critical for both designers and analysis engineers. In order to improve the interior noise performance, a good understanding of cabin vibro-acoustic characteristics is of critical importance to provide insights into the acoustic design and noise mitigation strategies.

Typically, the operator cabin is considered as a structural-acoustical system composed of an acoustic enclosure surrounded by flexible panels that are bonded to the cab frames. Therefore, the interior sound field is significantly affected by the acoustic cavity resonances, panel vibration modes and the panel-cavity interaction. In this study, the cabin acoustical characteristics are investigated using analytical solution, FEA calculation, and *in-situ* experimental analysis, respectively. As the analytical solution is based on the assumption of a rigid-walled cavity, it does not account for the panel-cavity coupling effect, which could lead to a remarkable predicting discrepancy from the real acoustical characteristics. In comparison with the analytical solution, FEA employs the modal coupling theory to accommodate the structure-acoustic interaction in modeling the acoustic cabin cavity. However, the model coupling approach has two main limitations in that it is only suitable for weak coupling and it does not satisfy the basic requirement of velocity continuity on the panel-cavity coupling interface. In contrast to simulation, the experimental acoustic modal analysis provides more meaningful information in characterizing the realistic vibro-acoustic behavior of the cab cavity *in-situ*. Hence it continues to be used as a practical troubleshooting tool and

---

H. Xu (✉) • J. Wang • H. Kang  
Virtual Product Development, Volvo Construction Equipment, Shippensburg, PA 17257, USA  
e-mail: [hongan.xu@volvo.com](mailto:hongan.xu@volvo.com)

O. Dickinson  
Operator Platform and Environment, Volvo Construction Equipment, Shippensburg, PA 17257, USA

an informative benchmark for modal correlation. Especially, a local vibro-acoustic behavior that is induced by a panel resonance can be easily identified via an acoustic mapping of the interior sound field. This case scenario will be examined in the following discussion.

Good efforts have been made in recent studies to improve the prediction accuracy of acoustic cavity modal characteristics. Pan and Bies [1] conducted an excellent review on the coupled structural-acoustic system composed of an acoustic space and a flexible wall surface. Du, Li and Xu, etc. [1, 2] proposed a general Fourier series method predicting the acoustical behavior of a rectangular cavity with arbitrary impedance boundary conditions. This method not only accounts for the non-uniform boundary conditions, but also allows a truthful enforcement of the velocity continuity condition on or near the fluid–structure interface. Sanderson and Onsay [4] carried out an experimental acoustic modal analysis aiming to investigate the impact of the flexibility of cab panels and the addition of seats on changing acoustic frequencies and mode shapes. Kavarana and Schroeder [5] proposed a modified FEA method to improve the vibro-acoustic cavity modal correlation. They utilized an omni-directional sound source to duplicate the test scenario and scale the relative amplitudes of vibro-acoustic modes using acoustic transfer functions from the measured locations. Tsuji, Enomoto and Maruyama etc. [6] attempted to improve the simulation accuracy by utilizing the experimental acoustic mode shapes that determine the detailed sound pressure distribution at the coupled interfaces of the acoustic and structural system. Mamede, Varoto and Oliveira [7] investigated the vibro-acoustic coupling phenomena by using an experimental study of the interaction between acoustic and structural modes for a vehicle interior cavity for the low frequency range. Specifically, they focused on the extraction of cavity modal properties from measured acoustic-structural FRFs. Cherng, Bonhard and M. French [8] studied the influence of the seat orientation and trimmed material properties on the acoustic cavity modal behaviors using a mock-up passenger compartment.

One of the motivations for the investigation detailed in this report was the incidence of booming noise in a SD upgrade compactor [9]. The booming noise was perceived as a deep resonant sound with a significant increase in the sound pressure level (SPL) measured at the operator’s ear position while the drum spins at 2,025 rpm. In order to identify the root cause(s) of the booming noise, an extensive experimental NVH investigation was carried out. As a key part of booming noise trouble shooting process, the acoustic cavity modal analysis not only helps the root cause identification, but also benefits the FEA prediction for the virtual Cab NVH development at early design phases. The objective of this work mainly focuses on but is not limited to:

1. Revisit the feasibility of using a rigid-walled acoustic cavity to approximate its *in-situ* counterpart in terms of modal characteristics.
2. Examine the impact of the seat and steering column on changing acoustic modal frequencies and mode shapes.
3. Investigate the local vibro-acoustic behavior and its relation to the low frequency compactor booming noise.

## 22.2 Analytical Acoustic Description of a Cavity

At early design stage, the cabin acoustic modes can be approximately determined using analytical solutions for a rigid-walled rectangular cavity. Figure 22.1 depicts a rectangular acoustical cavity of dimensions  $L_x \times L_y \times L_z$  with an associated coordinate system.

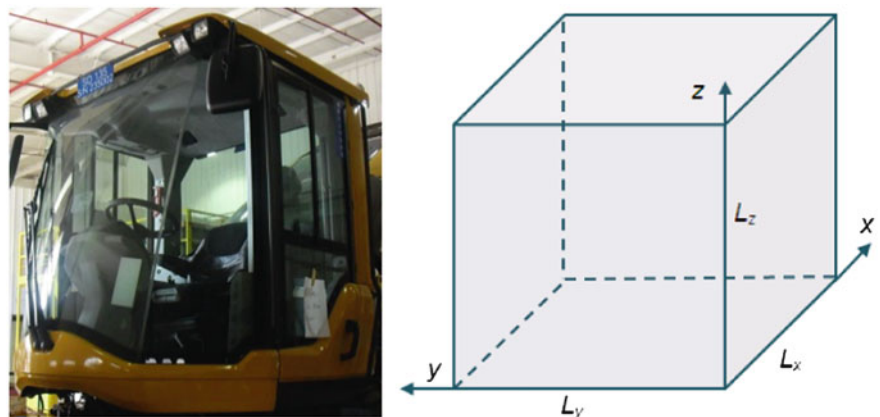
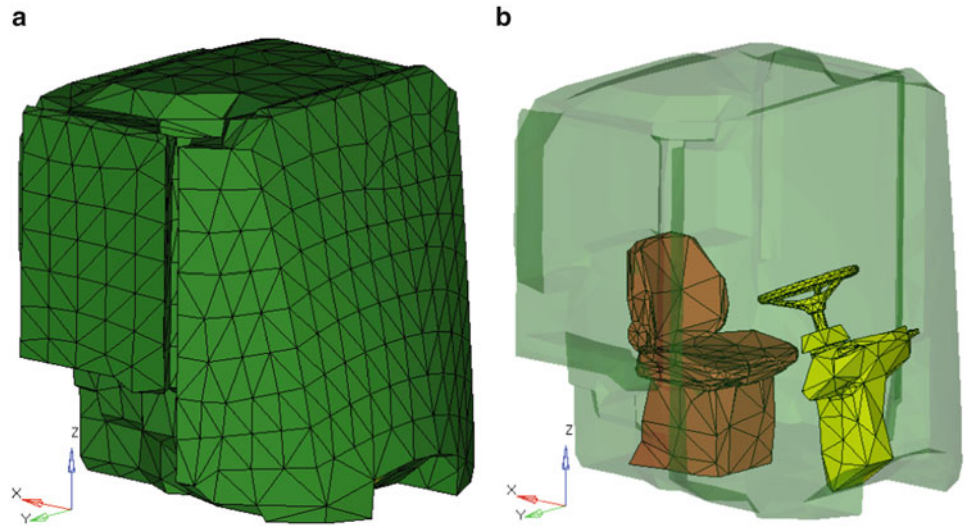


**Fig. 22.1** ISO view of the cabin and its equivalent box dimensions

**Fig. 22.2** FE cavity model:  
 (a) no seat and steering column;  
 (b) with seat and steering column



The exact values for the natural frequencies of a rigid-walled rectangular cavity are well known as:

$$f_n = \frac{c_0}{2} \sqrt{\left(\frac{n_x}{L_x}\right)^2 + \left(\frac{n_y}{L_y}\right)^2 + \left(\frac{n_z}{L_z}\right)^2} \quad (22.1)$$

where  $c_0$  is the speed of sound,  $L_x$  is the depth,  $L_y$  is the width, and  $L_z$  is the height of the cavity. In addition,  $n_x, n_y$  and  $n_z$  denote the modal orders in  $x, y$  and  $z$  directions, respectively. The modal functions for rigid-walled rectangular cavity are simply the products of cosine functions in three dimensions:

$$\Psi_{n_x n_y n_z} = \cos \cos \lambda_{n_x} x \cos \cos \lambda_{n_y} y \cos \cos \lambda_{n_z} z \quad (22.2)$$

where  $\lambda_{n_s} = n_s \pi / L_s$  ( $s = x, y, \text{ or } z$ )

In this case,  $L_x = 1.34m$  and is measured as the average distance between the front windshield to rear window,  $L_y = 1.54m$  and is the distance between two side windows, and  $L_z = 1.75m$  is the height of the cavity measured from floor to roof.

### 22.3 FEA Calculation

FEA is also commonly used at early design phase to predict the fundamental trends of the acoustical cavity. Fig. 22.2 shows the FE acoustic cavity being modeled with and without steering assembly and seat. The 2nd order solid tetra elements were used to mesh the cavity. The entire cavity mesh consists of 15,000 elements with an average size of 80 mm. By accommodating the real geometry layout, FEA is more accurate than analytical solution in predicting rigid-walled cavity acoustical behavior. Even though the rigid-walled assumption is not realistic due to the fact that the actual cabin consists of a number of flexible panels, the rigid-walled acoustic modes still provide a benchmarking for investigating the acoustic modal difference due to the structure-acoustic interaction. Therefore, the rigid-walled cavity model will be utilized in the following case study.

### 22.4 Physical Acoustic Cavity Characterization

Two testing cases were performed on the cab shell with and without the seat and steering column, respectively. The cab was settled on two airbags to simulate a free-free boundary condition, shown in Fig. 22.3a. A low frequency omni-directional volume velocity sound source was used to excite the cab cavity. The source was placed at the front left corner of the cavity and isolated with soft foam from the cab body as shown in Fig. 22.3b. A white noise signal from 20 to 500 Hz was used as the driving signal to excite the acoustic modes of interest. Figure 22.4 illustrates the acoustic instrumentation. An array consisting of 6 microphones spanned the interior and was moved along the depth (front to rear) and height (floor to roof) of

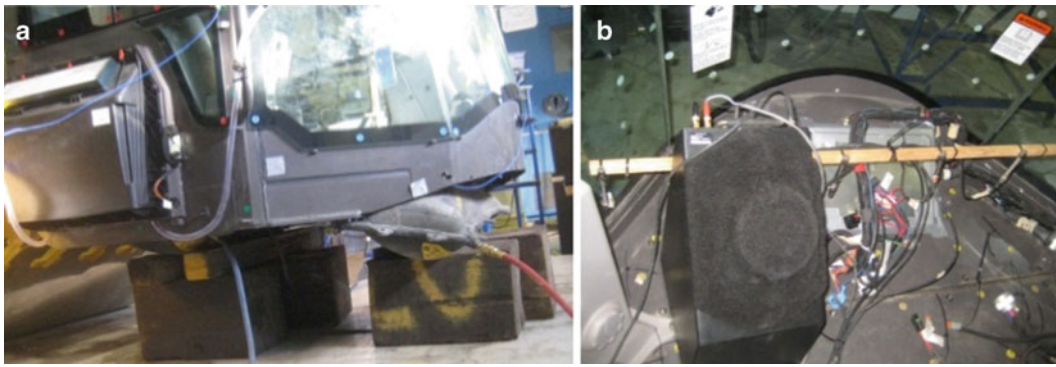


**Fig. 22.3** (a) Completely detached cab shell sitting on airbags; (b) omni-directional volume velocity sound source

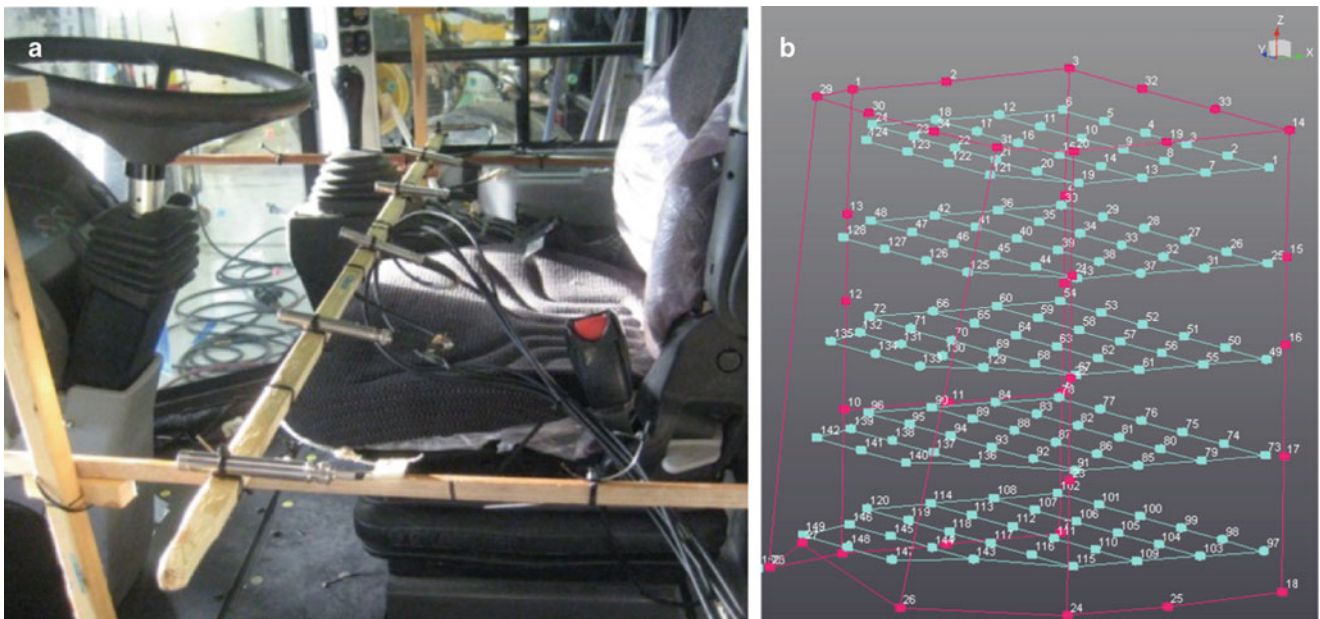


**Fig. 22.4** (a) Microphone array setup; (b) measurement grid

the cab which defined a measurement grid. Two wooden strips extending from the front to the rear of the cab support the moving microphone array. The vertical wooden frames were used to raise and lower the moveable array throughout the space. The acoustic transfer functions ( $P/Q$ ) were measured between microphone responses at all grid points with respect to the volume velocity of the source. The acoustic modal parameters were extracted using PolyMAX method.

## 22.5 Results and Discussion

### 22.5.1 Feasibility of Rigid-Walled Assumption in Predicting Acoustic Cavity Modal Characteristics of the Cab In-Situ

The rigid-walled assumption is frequently used to estimate the cab cavity resonances by design engineers at early cab development stage. However, the level of accuracy for this approximated prediction is rarely examined due to the lack of a comprehensive experimental benchmark. This session is aiming at filling this void by quantitatively investigating the feasibility of rigid-walled acoustic cavity in approximating its *in-situ* counterpart in terms of modal characteristics.

Due to the fact that most challenging cab noise issues are in the low frequency range, for example, the booming noise, only 1D, 2D and the first 3D modes are considered. Table 22.1 shows the comparisons of the first 7 modal frequencies obtained by



**Table 22.1** Comparison of acoustic modal frequencies

Index			Analytical	FEA mode (Hz)	Test mode (Hz)	Analytical FEA Analytical		
$n_x$	$n_y$	$n_z$	mode (Hz)			vs. test	vs. test	vs. FEA (%)
0	0	1	1 97.2	1 115.9	4 112.1	-13.3	3.4	16.1
0	1	0	2 110.7	2 132.7	2 93.6	18.7	41.8	16.6
1	0	0	3 126.9	3 149.9	6 137.4	-7.6	9.1	15.3
0	1	1	4 147.3	4 185.3	7 171.7	-14.2	7.9	20.5
1	0	1	5 159.8	5 194.8	-	-	-	18.1
1	1	0	6 168.4	6 215.7	-	-	-	21.9
1	1	1	7 194.4	8 228.7	9 230.5	-15.6	-0.8	15.0

analytical solution, FEA and test. Note that the modal sequence achieved from test is quite different from the one predicted by analytical solution and FEA. For instance, the vertical mode (0, 0, 1) is the first mode in analytical solution and FEA but the fourth mode in test. Also, in test the vertical mode (0, 0, 1) comes after the lateral mode (0, 1, 0) whereas in analytical solution and FEA the sequence of these two modes is switched. In addition, the natural modes given by test are slightly lower compared to the FEA prediction. This is because the flexibility of panels surrounding the cavity results in an “elastic” acoustical boundary condition hence making the cavity acoustically longer than the physical dimensions [4]. For the cab *in-situ*, the side panels are made of glass whereas the roof and floor are steel, therefore the cavity wall is softer laterally but stiffer vertically, which makes the cavity acoustically longer in lateral direction ( $y$ -axis) than the vertical direction ( $z$ -axis). It is also noticed that modes (1, 0, 1) and (1, 1, 0) are missing in test, which is due to the elastic cavity wall as well. The prediction accuracy of analytical solution and FEA can be measured by the percentage discrepancy against experimental results. The accuracy level of analytical prediction is between 80 and 90 % and the one of FEA prediction is as high as 90 % except for the 2nd mode (0, 1, 0) which has a 40 % predicting deviation.

The mode shapes associated with Table 22.1 are plotted in Fig. 22.5. Note that FEA and test have a nearly perfect match for 1D and 2D modes and a reasonable agreement for the first 3D mode (1, 1, 1). It should be emphasized once again that the experimental modal sequence needs to be adjusted to match the counterpart mode shapes given by analytical solution and FEA. Besides, a fairly reasonable agreement is found between analytical solution and FEA, especially in the case of 1D and 2D modes. This implies that the geometrical deviation between an FE model and its equivalent rectangular box is not so significant in predicting the lower order acoustic cavity mode shapes.

Figure 22.6 depicts the unique testing modes that are not listed in Table 22.1. Note that the first mode in test is a longitudinal mode (1, 0, 0) at 79.7 Hz in  $x$ -axis, shown in Fig. 22.6a. The third testing mode shown in Fig. 22.6b is a *quasi*-vertical mode in  $z$ -axis meaning a transition mode between the 2nd lateral mode and the 4th vertical mode. Figure 22.6c, d present the modes in such a way that they can be somewhat treated as a (0, 0.5, 0.5) mode and a (1, 0.5, 0.5) mode, respectively. Again, these unique modes can be attributed to the vibro-acoustic coupling effect between the air cavity and the flexible cab panels.

### 22.5.2 Impact of the Seat and Steering Column on Experimental Acoustic Modal Parameters

The addition of the seat and steering column introduces a mass coupling effect to the interior sound field which could generate a substantial impact on the cavity acoustic behaviors [8].

Table 22.2 shows the acoustical natural frequencies and modal damping that were extracted from measurements with and without the addition of the seat and steering column. The first observation is that the modal frequencies are uniformly shifted downwards by 1–5 % after adding the seat and steering column. Particularly, the vertical mode #4 shifts more to the lower value than the lateral mode #3 and the longitudinal mode (mode #5 for with seat and mode #6 for no seat). The addition of the seat and steering column causes a little frequency shift for the 3D mode (1, 1, 1), which is a combination of longitudinal, lateral and vertical mode.

However, the results are counter intuitive because the interior volume of the cavity decreases with the addition of the seat and steering column, which should increase the modal frequencies. The same observation was found in previous publications [4, 8].

In order to further investigate the acoustic modal behavior, a sum block of measured acoustic transfer functions ( $P/Q$ ) is plotted in Fig. 22.7 for the two cases. The sum block is essentially an averaged response of acoustic transfer functions measured at all microphone locations, which is useful to identify the modes as well as the relative strength of modes. The averaged acoustic transfer function shows that the two cases generally share a similar trend in terms of peaks and valleys in the frequency range of interest except for the mode at 121.2 Hz, which is absent with the addition of the seat and steering

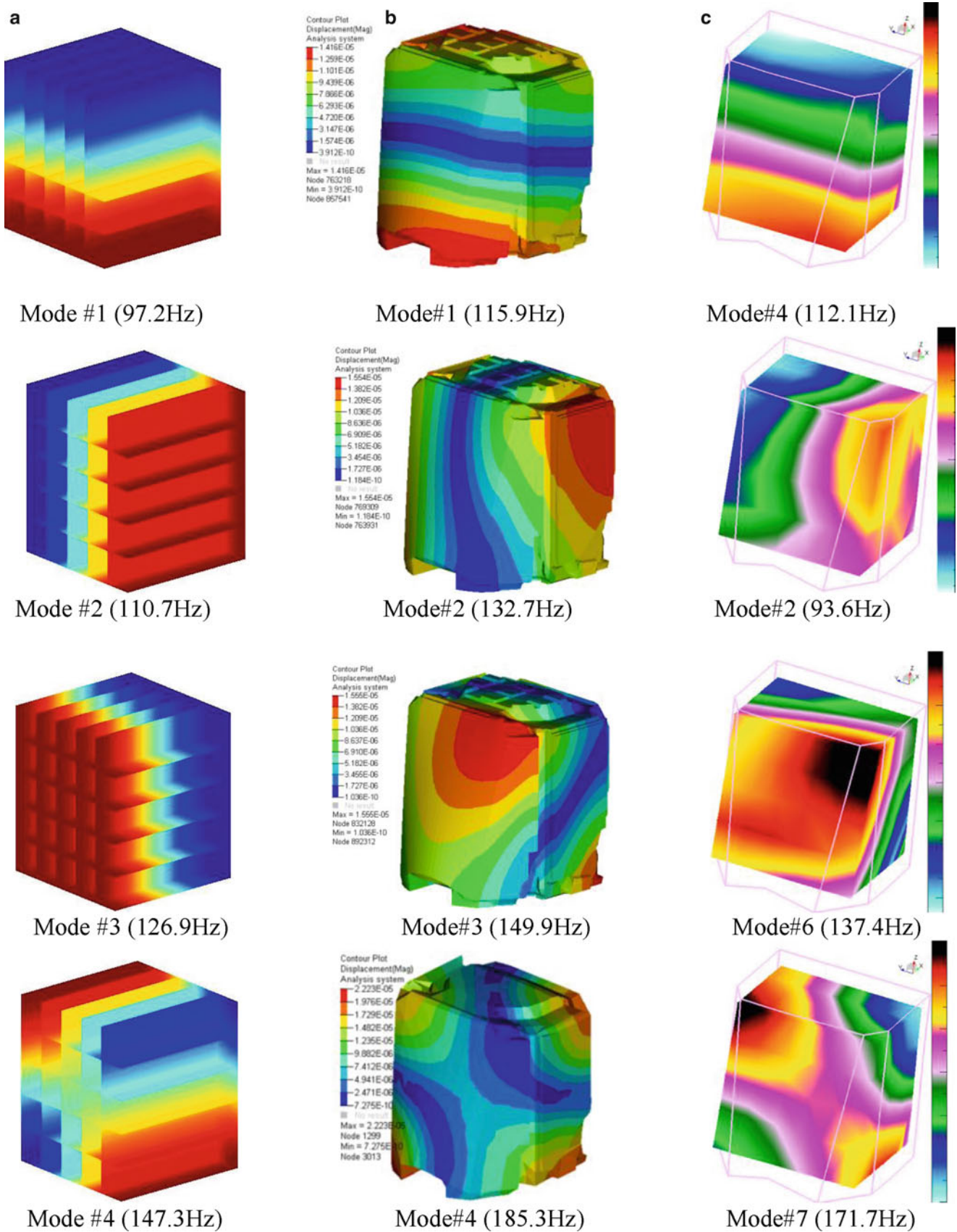


**Fig. 22.5** Comparison of cavity mode shapes: (a) analytical solution; (b) FEA; (c) test

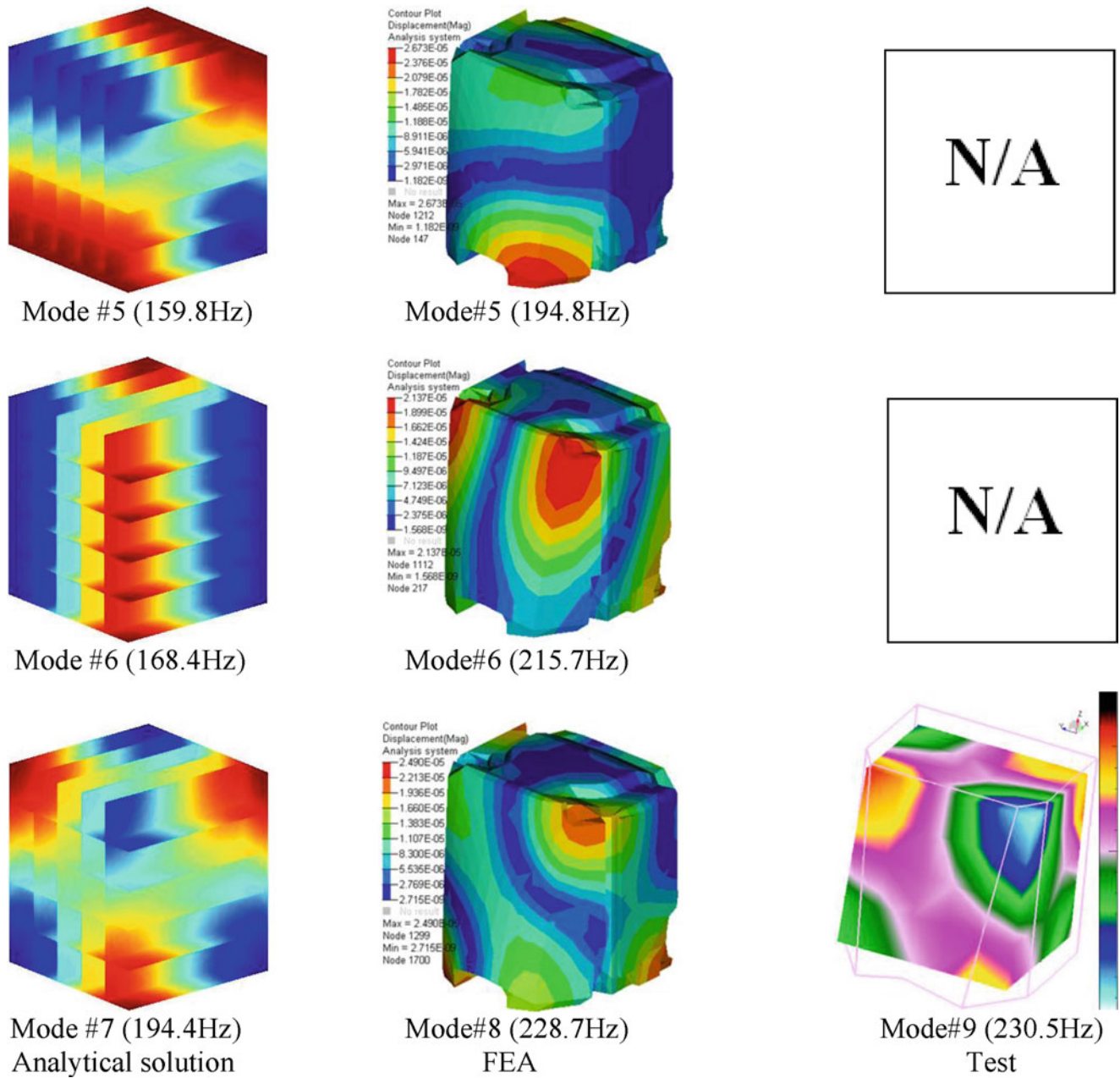
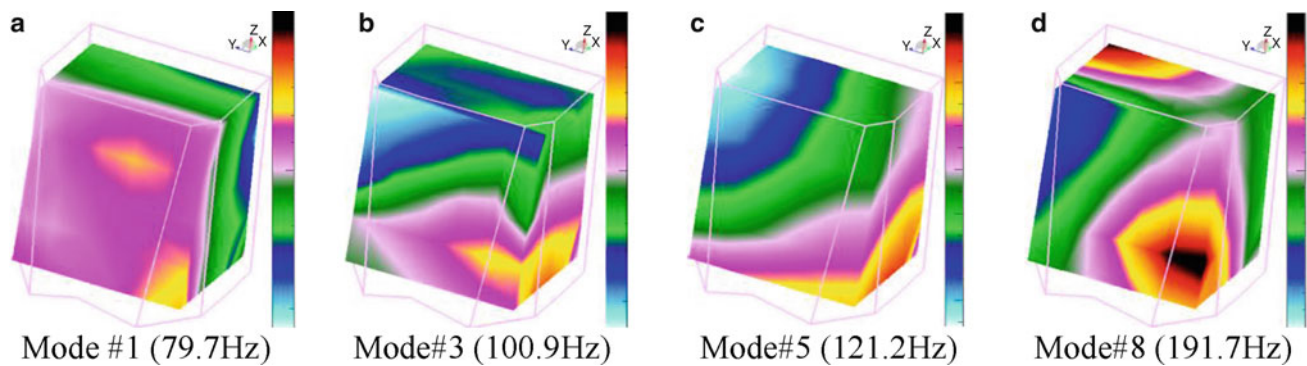


Fig. 22.5 (continued)

column. It is also noted that the modal response increases with the addition of the seat and steering column. Regarding the relative strength of modes, the vertical mode #4 is the most dominant one for both cases. In practice, this vertical mode may induce high sound pressure levels if it is coincident with excitation frequencies such as the engine firing orders. Such a mode should be precisely identified from the FEA model prior to the physical prototype to facilitate the cab NVH development.

The corresponding mode shapes are compared in Fig. 22.8. Note that when the seat and steering column are added, the vertical mode #4 somehow tends to start coupling with a lateral mode in y-axis. For the longitudinal mode #6, the region where the maximum pressure response concentrates migrates from the front top left corner to the front bottom right corner.



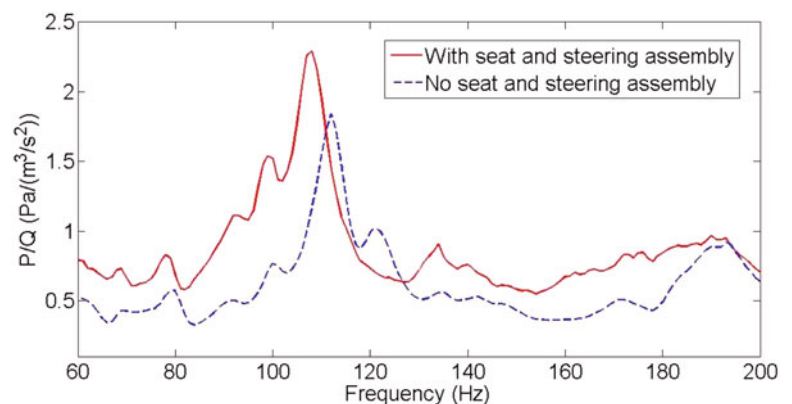


**Fig. 22.6** Experimental vibro-acoustic cavity modes missed in theoretical and FEA prediction

**Table 22.2** Comparison of acoustical natural frequencies and damping extracted from measurements with and without seat and steering column

With seat and steering column			No seat and steering column			Frequency difference (%)
Mode	Frequency (Hz)	Damping (%)	Mode	Frequency (Hz)	Damping (%)	(No seat–with seat)/no seat
1	79.1	0.4	1	79.7	1.7	0.8
2	92.8	1.1	2	93.6	1.8	0.9
3	99.3	1.1	3	100.9	0.9	1.6
4	108.1	3.5	4	112.1	2.6	3.6
–	–	–	5	121.2	2.5	–
5	135.1	3.9	6	137.4	3.2	1.7
6	164.1	1.8	7	171.7	2.3	4.2
7	190.7	1.52	8	191.7	2.2	0.5

**Fig. 22.7** Comparison of block ATF with and without seat and steering column



### 22.5.3 Local Vibro-Acoustic Behavior and Its Relation to the Low Frequency Booming Event

As previously mentioned, one of the motivations of this study is to help identify the root cause of a low frequency booming noise on a compactor. The booming noise was perceived as a deep resonant sound at the operator's ear position at 34 Hz. The cab dimension of  $1.34 \text{ m} \times 1.54 \text{ m} \times 1.75 \text{ m}$  indicates that the lowest flexible acoustic mode would be around 100 Hz which is much higher than the booming frequency. Besides, the initial diagnostic test subjectively found that the noise level remains almost the same regardless of positions. It implies that the noise is neither related to a standing wave nor a cavity mode. Based on the aforementioned facts, the booming event is therefore suspected to be due to a local vibro-acoustic response that could be induced by a cab panel resonance.

Figure 22.9 plots the averaged acoustic transfer function for the case with no seat and steering column in a range of 30–200 Hz. Note that there is peak at approximately 35 Hz dictating the entire frequency range. This peak, however, is actually related to a local panel resonance instead of a cavity mode, which can be verified through plotting the imaginary part of all measured acoustic transfer functions, as illustrated in Fig. 22.10.



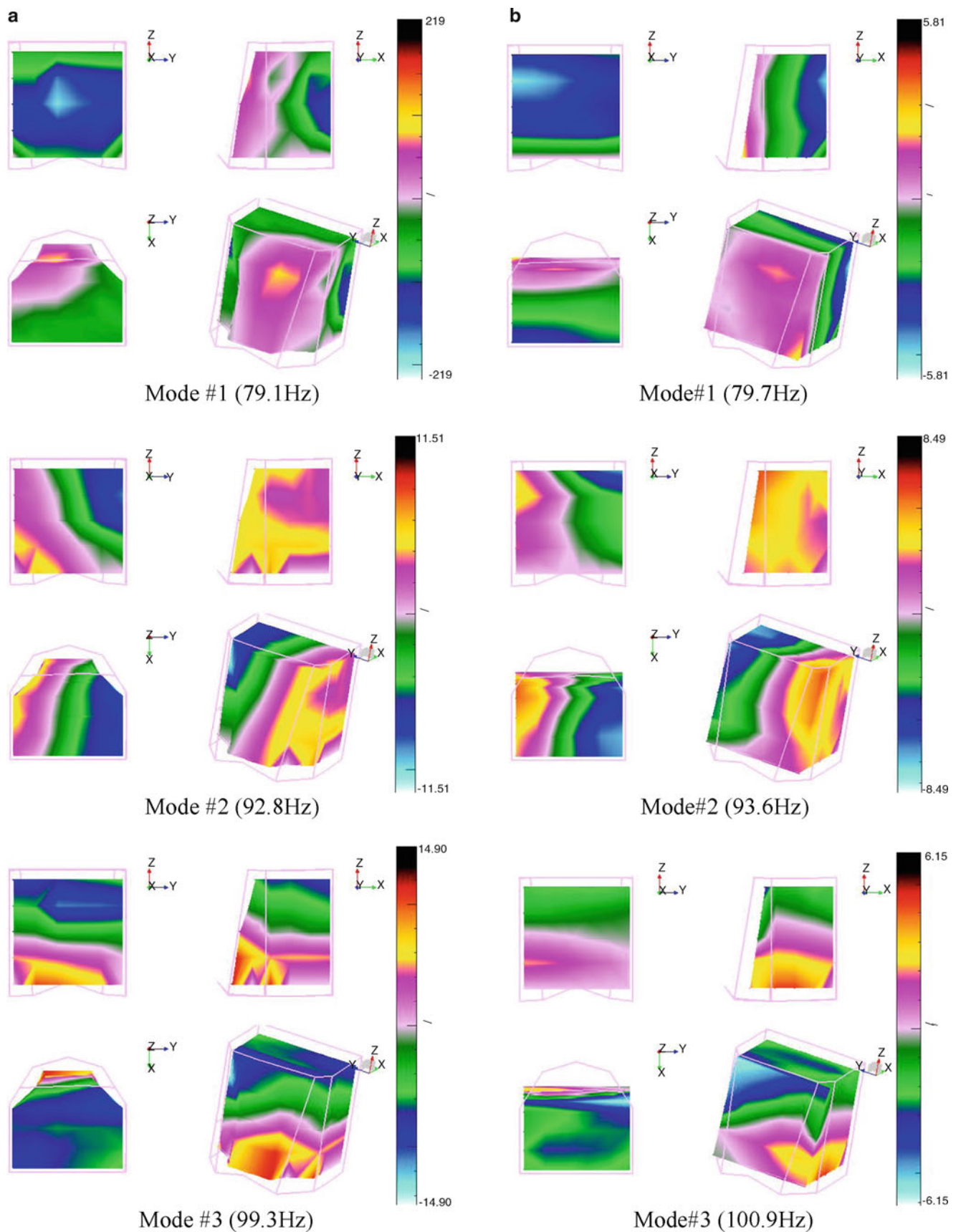


**Fig. 22.8** Comparison of experimental cavity modes with (a) and without (b) seat and steering column. (a) With seat and steering column (b) No seat and steering column

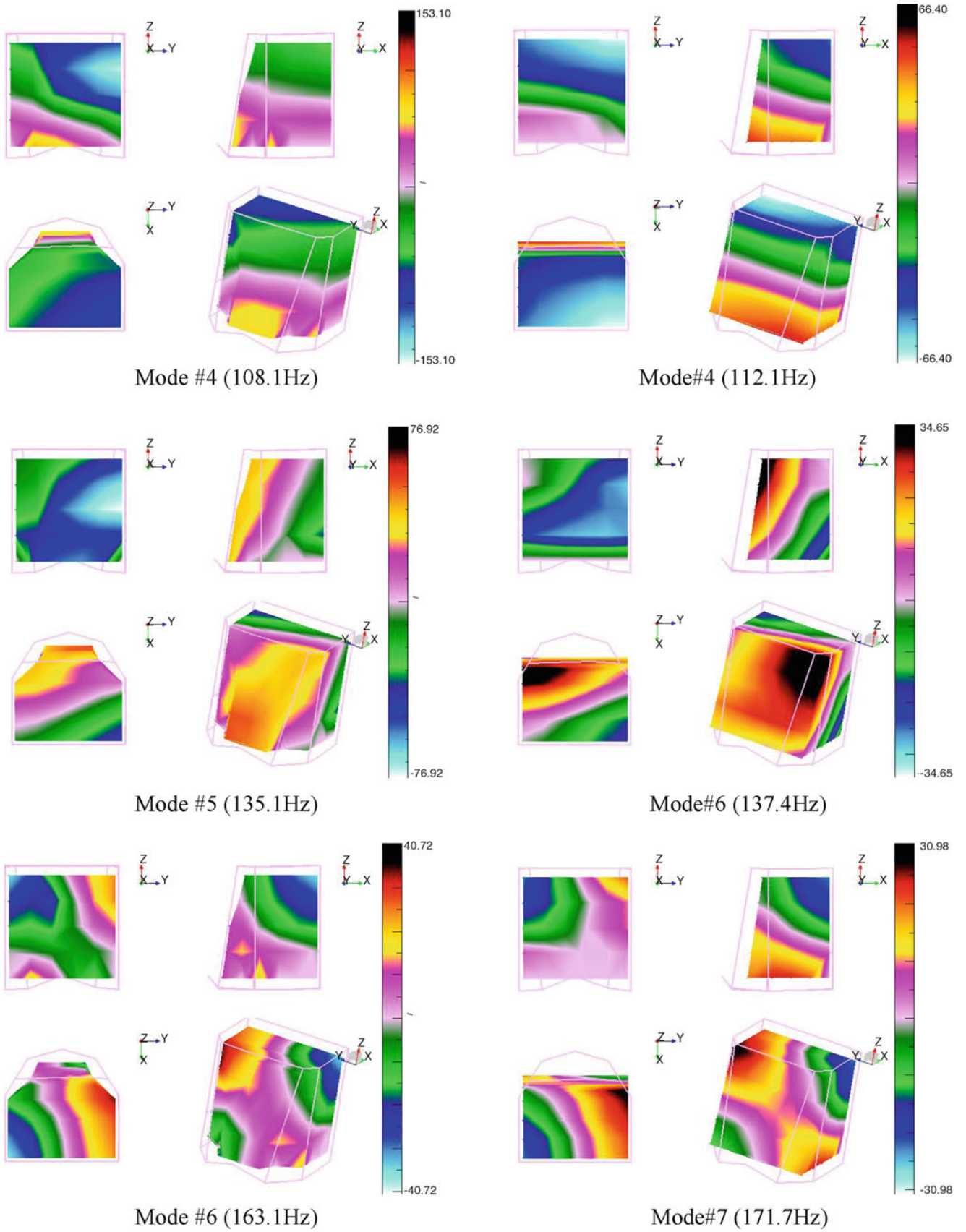


Fig. 22.8 (continued)

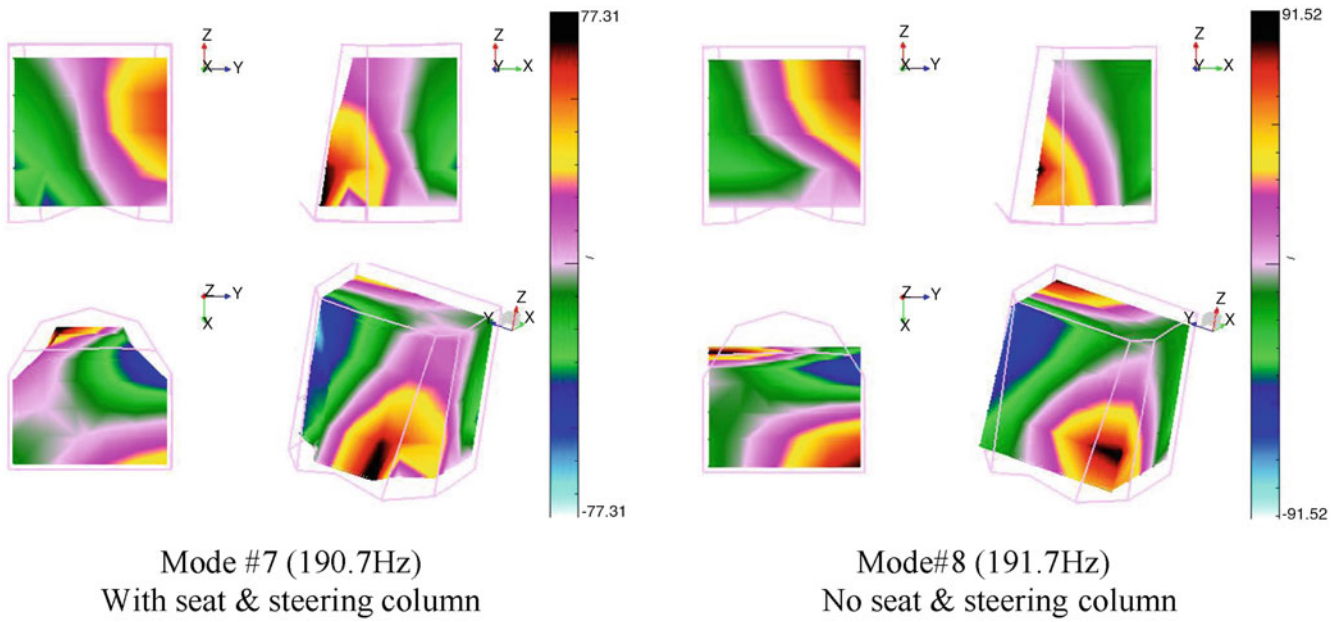


Fig. 22.8 (continued)

Fig. 22.9 Averaged acoustic transfer function with no seat and steering column

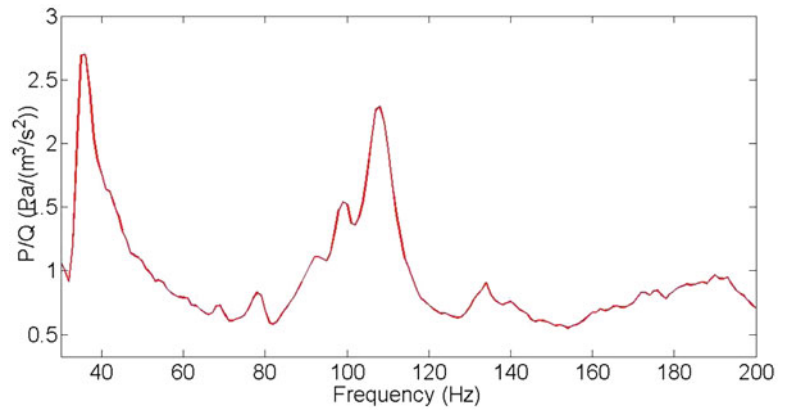
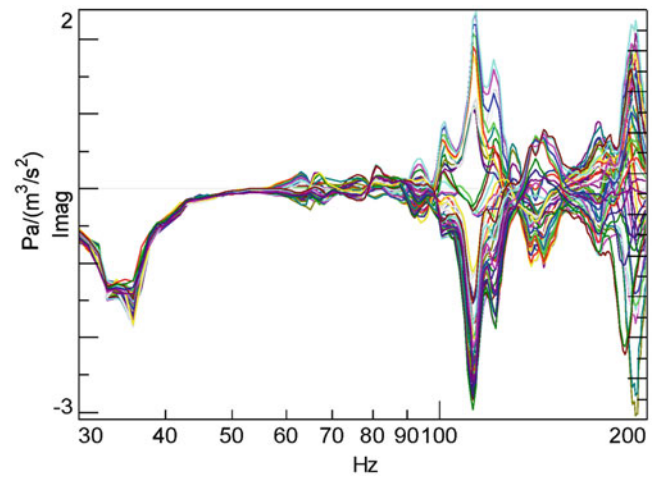
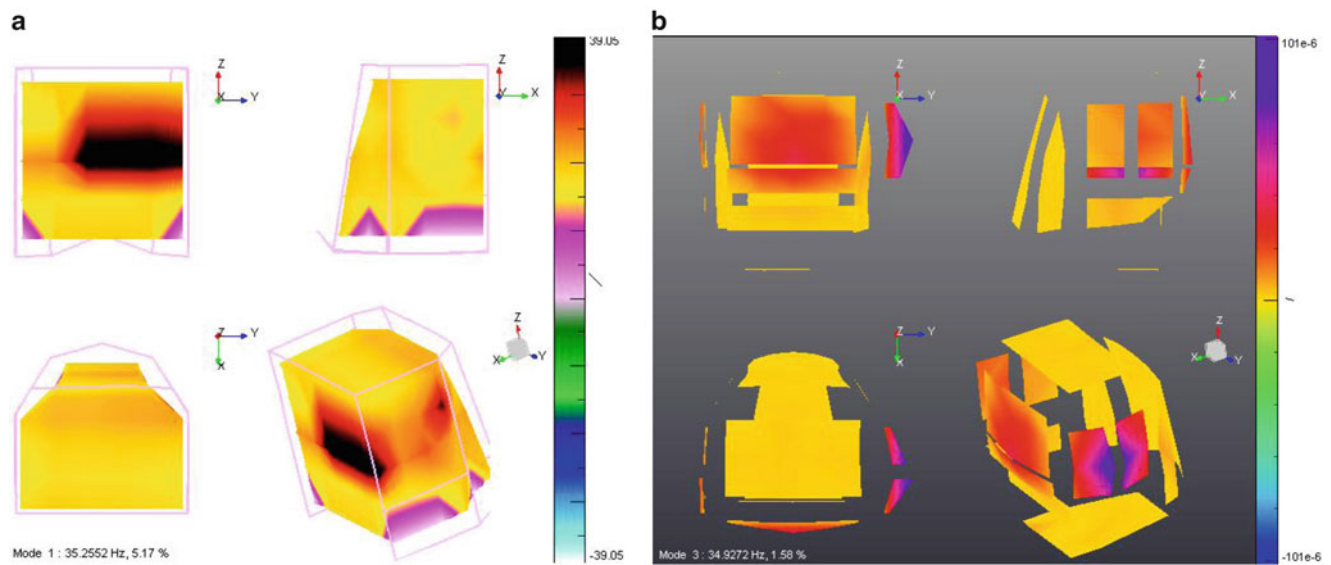


Fig. 22.10 Imaginary part of the acoustic transfer functions measured at all microphone locations







**Fig. 22.11** Illustration of a local vibro-acoustic behavior caused by a panel resonance 35 Hz. (a) Contour of pressure distribution at 35 Hz (b) Cab structural mode at 35 Hz

By definition, the imaginary parts of the frequency response functions for each modal frequency represent the associated mode shape. Particularly, to identify an acoustic mode, a sign change in the imaginary parts is essentially required. It is clearly showed in Fig. 22.10 that all the peaks of the imaginary parts point in the same direction. Thus we can conclude that the peak at 35 Hz is irrelevant to the acoustic cavity resonances.

To validate that the peak at 35 Hz is due to a local panel resonance, we conducted an experimental modal analysis on the cab structure. A structural mode was found at 35 Hz which is coincident with the booming frequency. For comparison, the structural mode shape is depicted together with an acoustic pressure mapping contour in Fig. 22.11. While the pressure distribution contour shows a high pressure concentration next to the rear and side windows, the structural mode shape indicates a local resonance of the rear and side panels accordingly. Apparently, the root cause of the booming noise is due to a local vibro-acoustic behavior that is initiated by the structural resonance of the rear and side panels. To suppress this local vibro-acoustic behavior, a practical countermeasure was implemented to shift the panel resonance away from the drum excitation frequency and the interior booming noise was tremendously attenuated.

## 22.6 Conclusion

The acoustic modal behaviors have been characterized qualitatively and quantitatively using analytical solution, FEA and experimental measurement. The primary findings and conclusions are summarized as below:

1. Based on the assumption of a rigid-walled cavity, the lower order modal frequencies predicted by the analytical solution and FEA differ 10–20 % and 10 %, respectively, from those obtained by tests. The experimental modal sequence is also quite different from the analytical and numerical ones. The prediction discrepancies are mainly attributed to the unrealistic rigid-walled assumption.
2. While the modal frequencies predicted by FEA and analytical solution have a deviation around 15–20 %, the predicted modal sequence is nearly the same. This could be due to the high irregularity of the cab geometry and the nearly identity 3D aspect ratio ( $x/y/z$ ) of cab dimensions.
3. Regarding the mode shapes, FEA and test have a nearly perfect match for  $1D$  and  $2D$  modes and a reasonable match for the first  $3D$  mode (1, 1, 1). Analytical solution and FEA have a reasonable agreement for the  $1D$  and  $2D$  modes. This implies that the geometrical deviation between an FE model and its equivalent rectangular box is not so significant in predicting lower order acoustic cavity mode shapes.
4. The addition of the seat and steering column shifts the modal frequencies down to lower values by 1–5 % but makes a little difference to the mode shapes.

5. The averaged acoustic transfer function ( $P/Q$ ) plays an important role in determining the relative strength of acoustical modes.
6. The local vibro-acoustic behavior is of critical importance in affecting the interior sound field. The root cause of the local vibro-acoustic behavior is attributed to the panel resonances.

## References

1. Pan J, Bies DA (1990) The effect of fluid-structural coupling on sound waves in an enclosure—theoretical part. *J Acoust Soc Am* 87(2):691–707
2. Du JT, Li WL, Liu ZG, Xu HA, Ji ZL (2011) Acoustic analysis of a rectangular cavity with general impedance boundary conditions. *J Acoust Soc Am* 130(2):807–817
3. Du JT, Li WL, Xu HA, Liu ZG (2002) Vibro-acoustic analysis of a rectangular cavity bounded by a flexible panel with elastically restrained edges. *J Acoust Soc Am* 131(4):2799–2810
4. Sanderson MA, Onsay T (2007) FEA interior cavity model validation using acoustic modal analysis. SAE Technical Paper 2007-01-2167
5. Kavarana F, Schroeder A (2012) A practical FEA approach to determine acoustic cavity modes for vehicle NVH development. SAE Technical Paper 2012-01-1184
6. Tsuji H, Enomoto T, Maruyama S, Yoshimura T (2012) A study of experimental acoustic modal analysis of automotive interior acoustic field coupled with the body structure. SAE Technical Paper 2012-01-1187
7. Mamede WF, Varoto PS, de Oliveira LRP (2002) Vibro-acoustic modal testing of a vehicle cabin, Proceedings of the 27th International Seminar on Modal Analysis (ISMA 27), 2002
8. Cherng J, Bonhard RB, French M (2002) Characterization and validation of acoustic cavities of automotive vehicles. *Soc Photo Opt Instrum Eng* 1:290–294
9. Xu H, Wang J, Owen D, Kang H (2013) Experimental vibro-acoustic analysis for troubleshooting compactor cab booming noise. In: Proceedings of Noise-Con 2013, August 26–28, Denver, CO